RSC Advances

ROYAL SOCIETY OF CHEMISTRY

www.rsc.org/advances

Cite this: DOI: 10.1039/c0xx00000x

www.rsc.org/xxxxxx

ARTICLE TYPE

Physical, structural, and dehydrogenation properties of ammonia borane in ionic liquids

Tessui Nakagawa,*[a,†] Anthony K. Burrell,[a,‡] Rico E. Del Sesto,[a,§] Michael T. Janicke,[b] Adam L. Nekimken,[c] Geraldine M. Purdy,[a] Biswajit Paik,[a,‖] Rui-Qin Zhong,[a,¶] Troy A. Semelsberger,[a] and Benjamin L. Davis*[a]

Received (in XXX, XXX) Xth XXXXXXXXX 20XX, Accepted Xth XXXXXXXXX 20XX
DOI: 10.1039/b000000x

Ionic liquids (ILs) are excellent solvents for the dehydrogenation of ammonia borane (AB). However, the basic properties that allow efficient dehydrogenation are still unclear. In this report, density, viscosity, melting/freezing/glass transition temperature, and solubility of AB-imidazolium-based IL solutions were studied as well as their dehydrogenation properties including impurity gas quantification. The ILs can solubilize 32~35 wt% of AB. The liquid AB-IL solutions have densities of ~0.9 g/cm^3, viscosities similar to motor oil (100~250 cP), and glass transition temperatures below –50 °C. AB-ILs are stable at room temperature for several weeks with minimal hydrogen generation, though some hydrolysis occurs immediately upon after mixing as a result of trace water content. More than 2 mol H_2/AB are desorbed from AB-ILs between 80~130 °C with limited impurity emissions. There is no reaction between AB and ILs upon dehydrogenation, and based on structural analysis results in a complex solid solution.

Introduction

Energy and green securities are acute global issues. Fossil fuels have historically been the main resources for energy, but they are becoming more precious and generate greenhouse gases contributing to global warming. Hydrogen has been a strong candidate for the alternative resources of fossil fuels because of its clean and sustainable natures.[1] Since gaseous hydrogen has low volumetric energy density and low ignition energy, the main issue for the practical use of both off- and on-board system is the establishment of cheap, compact and safe hydrogen storage techniques.[2] The U.S. Department of Energy (DOE) sets the technical goal for a storage system with a storage density of 5.5 wt%[3] and the minimum material-based target are 7.8 (liquid), 9.8 (solutions), and 11.2 wt% (slurries).[4]

Ammonia borane (AB) has been one of the frontrunners of hydrogen storage materials, especially for the lofty requirements of automotive applications. AB has two distinctive advantages: high hydrogen capacity (19.6 wt%) and moderate operating temperatures (<100 °C).[5] Neat AB desorbs hydrogen via an exothermic reaction, releasing two equivalents of H_2, and then third dehydrogenation of AB can occur at higher temperatures:[6]

$$NH_3BH_3 \rightarrow \text{“}NH_2BH_2\text{”} + H_2, \quad 6.5 \text{ wt\% below } 114 \text{ °C} \quad (1)$$

$$\rightarrow \text{“}NHBH\text{”} + 2H_2, \quad 13.1 \text{ wt\% below } 200 \text{ °C} \quad (2)$$

$$\rightarrow BN + 3H_2, \quad 19.6 \text{ wt\% over } 400 \text{ °C}. \quad (3)$$

There are a number of possible reaction paths of AB dehydrogenation, but “NH_2BH_2” and “NHBH” mainly are present as polymeric structures.[6] Unfortunately, neat AB has several issues limiting its utility including (1) slow dehydrogenation kinetics; (2) release of impurity gases (diborane, ammonia, and borazine) during dehydrogenation that are harmful to fuel cells; (3) lack of on-board regeneration, and (4) lack of existing pumpable forms (e.g. liquid states). Various approaches to overcome these issues have been performed for over a decade; for example, using catalysts,[7-9] Lewis and Brønsted acids,[10] metal hydride mixtures,[11,12] proton sponge activation,[13,14] nano-confinements,[15-17] metal-substitutions,[18-21] and so on. Among them, a liquid-based fuel, which is AB in a polar solvent, is a quite promising option.[22-24] The advantages of a liquid fuel include potential compatibility with existing technologies, which requires minimum changes to existing infrastructures. One recent development of AB solution has been demonstrated by using ionic liquids (ILs), especially imidazolium based compounds, which are used for acceleration of AB dehydrogenation.[22] As known, liquefaction or formation of eutectics proceeds when these reported imidazoliums are mixed with AB. However, a 50:50 weight ratio of AB-IL mixture, which has been reported previously in the literature, exhibits a slurry nature due to oversaturation in our preliminary studies. Therefore optimizing of AB concentration in ILs is necessary if it is to be used as a liquid fuel along with optimized dehydrogenation kinetics.

There are still many properties that remain to be fine-tuned in order to commercialize AB-IL as a liquid fuel. For their practical use, fully understanding their properties from both engineering and scientific views is required. Hence, basic AB-IL properties such as saturation solubility of AB in ILs, viscosity, density, melting/freezing/glass transition temperature, thermal stability at room temperature, dehydrogenation kinetics, impurity quantification, and structural properties were studied in this report. Imidazolium ILs, which are 1-ethyl-3-methyl-, 1-butyl-3-

methyl-, and 1-butyl-2,3-dimethylimidazolium chloride (EmimCl, BmimCl, and BmmimCl, respectively), were selected for a systematic investigation since these materials have similar structures (Fig. 1) and physical properties but slightly different interactions with AB that affect the catalysis.[25-27]

Experimental

AB was purchased from Aviabor (>97% purity). ILs (EmimCl (Aldrich), BmimCl, and BmmimCl) were synthesized or decolorized in our Lab with <1% of impurity amount based on the previous report.[28] These ILs were mixed with AB at RT. Water content of ILs has been tested by Kerl Fisher titration (KF; Mettler Toledo, C20 Compact Kerl Fisher Coulometer) using acetonitrile (Fisher Chemical, 42.8 ppm of water content).

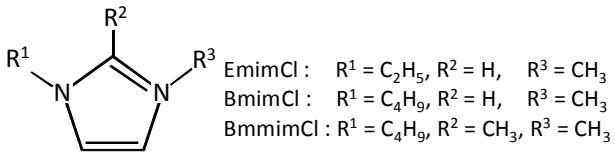

Figure 1. Structures of imidazolium-type ILs

The saturated solutions of AB-IL were prepared by mixing 50:50 wt% of AB and ILs for overnight and then removed unsolved AB by filtering. The density of each AB-IL solutions was determined by gravimetric analysis. Measured solution volume (0.5~0.9 mL) dropped on the balance was weighed by using 1 mL pipet. Each measurement was repeated 5~10 times and the average values are reported. Quantification of solubility was examined by ^{11}B solution NMR (Bruker, AVANCE 300, 96.29 MHz with 7.05 T) without solvent. Calibration curve of ^{11}B signal area was made by using tetraglyme/BF_3-etharate solution with known concentration (Fig. 2).

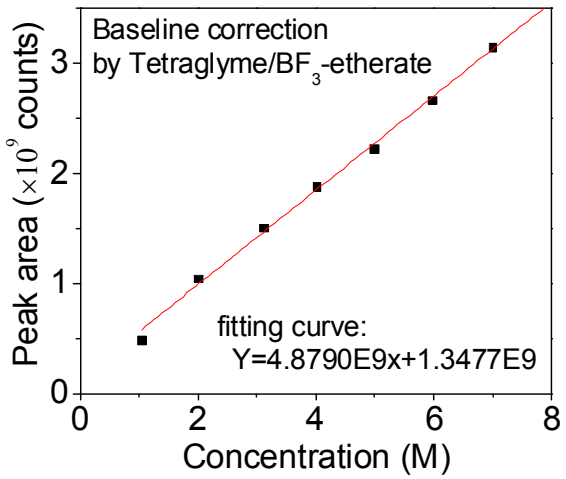

Figure 2. ^{11}B NMR calibration curve for boron concentration using tetraglyme/BF_3-etherate mixture.

Viscosity of AB-ILs has been measured by viscometer (Cambridge Viscosity, Viscolab 3000 viscometer). Melting/freezing/glass transition temperature of ILs and AB-ILs was measured by using differential scanning calorimeter (DSC; Mettler Toledo, DSC822e). Sample was enclosed in aluminium cell and then cooled/heated with 2 ºC/min of ramp rate. Stability (Shelf-life) of AB-IL solutions was examined at room temperature (30 ºC) for 2 weeks by using Sieverts' method (MRS; Parr instrument company, 5000 Multiple Reactor System). Dehydrogenation reaction of AB-ILs at high temperature region was performed by LaboSys evo (SETARAM) DSC with 1 ºC/min of ramp rate up to 170 ºC. Quantification of evolved NH_3, H_2, diborane, and borazine from AB-ILs have been carried out with 1 ºC/min of ramp rate up to 170 ºC by the thermogravimetric analyzer (TG; Mettler-Toledo, TGA 851) coupled with infrared spectrometer (IR; Thermo Nicolet, Avatar 380 FTIR) and residual gas analyzer (RGA; Inficon, Transpector® CPM). Calibration curve in each gas species has been corrected using various gas concentrations. Softwares for quantification analyses were TP 32 (Inficon) for Hydrogen and TQ analyst and OMINIC (Thermo Niclet) for the others. The detection limits of NH_3/H_2, diborane/H_2, and borazine/H_2 are less than 2000, 400, and 20 ppm, respectively. Structural information of neat ILs, as-mixed AB-ILs, and dehydrogenated AB-ILs have been acquired by ^{1}H and ^{13}C solution NMR (300.13 MHz for ^{1}H and 75.5 MHz for ^{13}C) using acetonitrile as a solvent and ^{11}B and ^{13}C MAS NMR (Bruker, wide bore AVANCE 400, 128.32 MHz for ^{11}B and 100.58 MHz for ^{13}C with 9.4 T) with ^{1}H-decoupling. Almost all experiments, except TG-IR-RGA and high temperature DSC, have been operated without exposing samples to air for prevention of water absorption of ILs. Air exposure time of samples for the TGA-IR-RGA and DSC were typically less than 10 seconds under Ar flow.

Results and discussion

Physical properties

From an engineering point of view, solubility is important to maximize the potential utilization of AB as a fuel. At least 68.2 wt% AB of solubility is required to satisfy DOE solution material target (9.8 wt% H_2 when 2.2 mol of H_2 desorbs from a mol of AB).[29] All of the ILs here solvate more than 30 wt% of AB in capacity, which results in ~4.5 wt% of useful material-base capacity (Table 1); however, none of them exceeds the DOE target. They have similar material density. The longer branch in ILs, the larger amount of AB solves into ILs. While the density of neat AB is 0.78,[30] the densities of EmimCl, BmimCl, and BmmimCl are 1.136 (at 130 °C),[31] 1.08 (at 25 °C),[32] and 1.36 g/cm^3 (at 20 °C, determined by our laboratory using the same method as ref. 32), respectively. Their solution densities are significantly different from that of the weighted average of neat AB and the respective ILs, which is likely caused by the interaction between AB and ILs. The AB concentration (molar ratio) seems to exhibit a molecular mass or branch number/size dependency, presumably indicating interaction strength between imidazolium cation and Cl^- and/or molecular geometry giving space for AB to dissolve.[33]

Table 1. Physical properties of *saturated* AB-IL solutions.

Sample	AB concentration			Density (g/cm^3)	Available H_2 (wt% fuel)
	wt%	mol%	mol/L		
AB-EmimCl	35.2	72.1	9.86	0.86	5.06
AB-BmimCl	32.2	72.9	9.08	0.87	4.63
AB-BmmimCl	32.5	74.6	9.03	0.86	4.67

Based upon our results, the optimized AB concentration for liquid

formation and desirable engineering properties has been determined as 30 wt% (IL: 70 wt%, available H_2: 4.3 wt%) due to mixing time. It takes more than 1 hour to obtain higher concentration of AB-IL liquid fuels than 30 wt% of AB, which became eutectic liquids when mixed. These optimized mixtures show relatively low viscosities of 150-200 cP at room temperature (cf. motor oil SAE 30: 100 to 250 cP at RT).[34] The densities of the 30 wt% of AB-IL solutions (Table 2) are slightly higher density than the saturated AB-IL solutions (Table 1). These solutions gradually lost their fluidity with releasing hydrogen. They became sticky paste and finally solid after dehydrogenation of ~1 and ~1.5 eq. H_2, respectively.

Table 2. Physical properties of *30 wt%* AB-IL solutions.

Sample	Viscosity (cP)	Density (g/cm^3)
AB-EmimCl	154.4 (33.2 °C)	0.920
AB-BmimCl	159.2 (32.4 °C)	0.904
AB-BmmimCl	201.9 (33.2 °C)	0.891

Figure 3 shows melting/freezing/glass transition DSC curves for neat ILs and AB-IL solutions. Many ILs show a glass transition,[25] but the neat ILs in this study show defined melting points, which consistent with previous reports (EmimCl: 84 °C,[26] BmimCl: 65 °C,[26] BmmimCl: 96.8 °C[27]), but differ slightly due to different water content. Supercooling is evident on the cooling cycle of the molten ILs, as is typically seen in these materials (Fig. 3 (a~c)). The AB-IL mixtures do exhibit glass transitions rather than melting, and range from -50 to -65 ºC (Fig. 3 (d~f)). Thus the formation of the eutectics by mixing AB with ILs greatly improves their temperature range of the liquid state required for engineering applications, maintaining at least a liquid nature to well below 0°C.

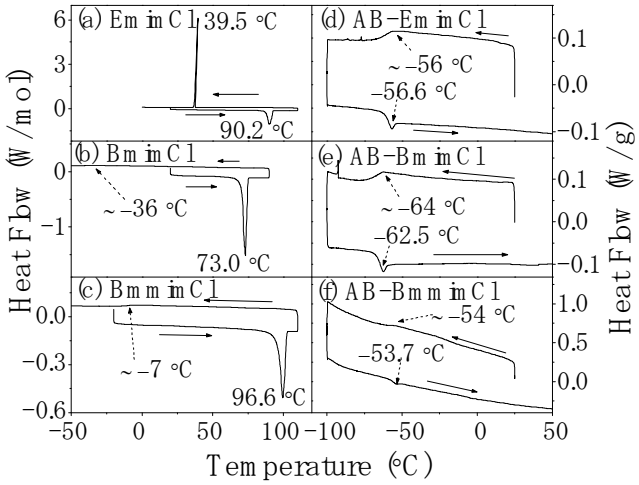

Figure 3. DSC curve of ILs and 30wt% of AB-ILs at low temperature.

Dehydrogenation properties

The stability of AB-IL liquid fuels at room temperature is an important factor for utilization so that the fuels have practical shelf-lives. AB normally does not dehydrogenate at room temperature. According to fig. 4, the AB-ILs dehydrogenated less than 0.09 mol H_2/AB over a period of 2 weeks, which is only 3.8% of total hydrogen capacity. Although this amount seems to be small in terms of fuel quality, the pressure in the tank can build up if free space in the tank is limited. For instance, in the case of a tank with 10 L of free space at 300 K, pressure builds up more than 100 bar if the fuel storing 5 kg H_2 desorbs 0.04 mol H_2/AB (fuel capacity used for calculation: 2.2 mol H_2/AB). Since this issue is comparable to a physisorption hydrogen storage system, installing a relief valve on the tank is necessary when they are used commercially. Water content significantly affects the stability of AB-ILs, as expected. When wet BmimCl (water content: 9500 ppm, determined by KF) is mixed with AB, hydrolysis between water and AB proceeds and the fuel loses ~0.08 mol H_2/AB within 24 hours (Fig. 4, dashed blue line).

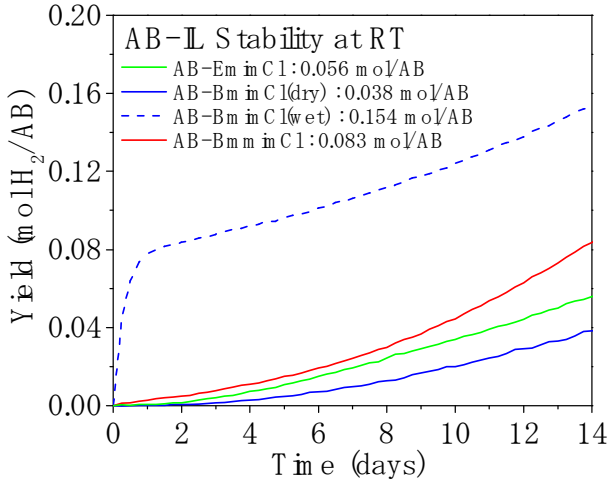

Figure 4. Thermal stability of 30 wt% of AB-ILs at room temperature.

Wet AB-BmimCl solution desorbs ~0.15 mol of hydrogen after 2 weeks although the dehydrogenation rate is approximately the same as the 'dry' ILs, suggesting that the water is consumed immediately upon mixing. Less than 50% of H_2 is lost when using dry ILs, such as dry BmimCl (water content: 29.8 ppm), EmimCl (54.8 ppm), and BmmimCl (118.1 ppm). Thus, to minimize water content in ILs is important for storing these fuels. Desorbed gases from each sample after the room temperature test in fig. 4 were analyzed by RGA-IR and their concentrations are listed in table 3. Surprisingly, AB-EmimCl and AB-BmimCl desorbed below the detection limit (BDL) of any impurity gas, which are the same hydrogen yield shown in fig. 4 and has tremendous implications in that these AB-IL mixtures are potentially impurity-free resource. Impurities can severely affect the performance of fuel cells, and they are often an issue in existing work related to AB as a fuel. The primary desorbed gas is hydrogen for all AB-IL mixtures, with a small amount of NH_3 (2.9 vol.% of total gas amount) and B_2H_6 (0.1 vol.% of total gas amount) detected when AB is decomposed in BmmimCl (Table 3). The difference with the latter IL may be due to the lack of the acidic (and hydrogen-bond capable) proton in the R^2 position of the imidazolium ring. The IL systems therefore have a strong advantage in terms of less amount of impurities which are harmful to the fuel cell. It is unclear what the mechanism is at this point, due to the extremely low concentrations that are being generated, if any at all. It is possible that the impurities from AB-IL solutions do generate impurities in the form of ammonia or various borane, but the ionic nature and polar components of the IL tend to readily solvate these gases,[35] while allowing the nonpolar H_2 to desorb readily as a highly pure gas. As most of the

poison impurities are fairly polar compounds, the IL has a significant advantage in suppressing gas impurity evolution over standard organic solvents. There is also a possibility that the IL somehow provides more control in the dehydrogenation kinetics of the AB, limiting the formation of impurities that can happen in the neat AB, as ILs have been shown to alter reaction kinetics in organic and organometallic chemistry, and it may occur here as well. In order to determine if this is the cause of the reduced impurities, however, would require a rigorous mechanistic study into the full dehydrogenation process of AB in the ILs and other solvents, which is currently in progress but beyond the scope of this report.

Table 3. Desorbed gas amount of AB-ILs after RT stability test. Detection limits: NH_3/H_2: <2000 ppm, B_2H_6/H_2: <400 ppm, and borazine/H_2 <20 ppm

Sample	H_2 (vol.%)	Borazine (vol.%)	B_2H_6 (vol.%)	NH_3 (vol.%)
AB-EmimCl	100.0	BDL	BDL	BDL
AB-BmimCl	100.0	BDL	BDL	BDL
AB-BmmimCl	97.0	BDL	0.1	2.9

Figure 5 shows TG-RGA-IR profiles with their respective DSC curves of AB-IL at ramping temperatures.

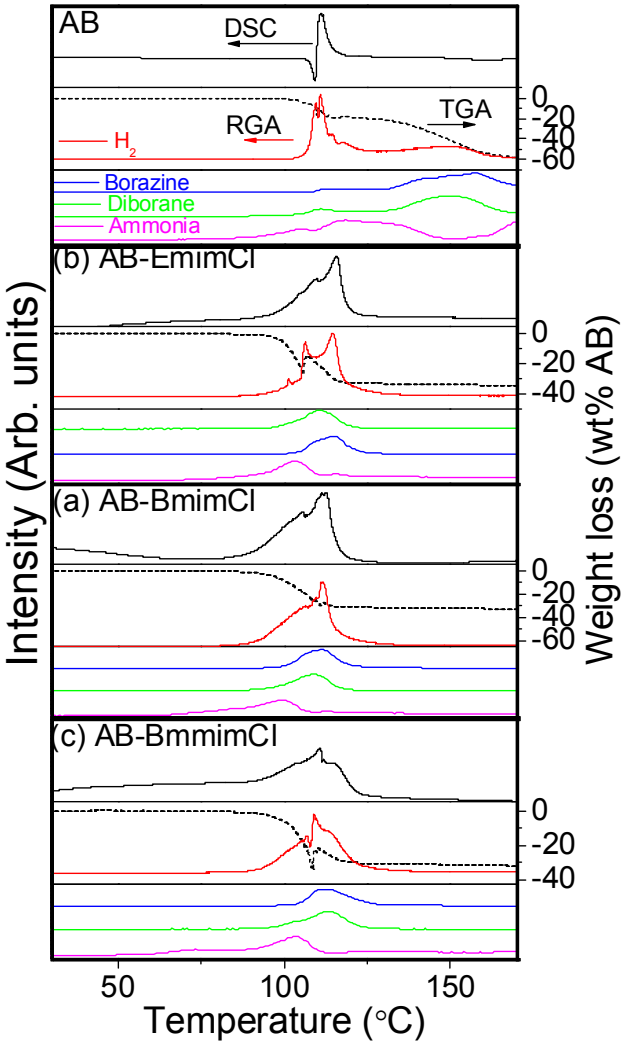

Figure 5. TG-RGA-IR and DSC profiles of AB-ILs decomposition.

AB dehydrogenates exothermically at ~110 °C after melting (endothermic signal) with a ramp rate of 1 °C/min. A second exothermic dehydrogenation occurs at ~150 °C, but the signal from an endothermic borazine evaporation overlays this exothermic signal due to the open cell used in this study (Fig. 5 (a)). In addition to the H_2, the first dehydrogenation results in ammonia emission, followed by the emission of borazine and diborane at the second dehydrogenation. AB-ILs used in this study show similar dehydrogenation temperature range with a peak at ~110 °C of hydrogen and exothermic signal, suggesting that their reaction mechanisms are similar. The second dehydrogenation step has completed below 130 ºC in all samples, as almost no weight loss or gas desorption are evident in AB-ILs above 130 ºC. Considering that the borazine and diborane were observed after NH_3 desorption, dehydrogenation steps of AB-ILs likely proceed in the same way as that of neat AB. The concentrations of the desorbed gases from AB-ILs are listed in table 4. All AB-ILs significantly decreased the amount of NH_3 and diborane impurities, but borazine was not suppressed. Other gas species such as mono-aminoborane[6] also have been dramatically suppressed and do not appear in our experiments. Compared with gas analysis after RT dehydrogenation test in table 3, borazine concentration is significantly higher than the RT dehydrogenation. This result can be explained in three ways: 1) dehydrogenation reaction at RT is the first dehydrogenation step; 2) low vapour pressure of borazine at RT; and 3) IL can trap many polar gases and capacity at RT is higher than that at higher temperature.[35] After dehydrogenation, these solutions became white solid, which is consistent with previous study.[22] Since solid spent fuel seems not favorable in terms of handling, finding a suitable IL to keep liquid state after dehydrogenation is important for the future work.

Table 4. Quantification of desorbed gas from AB-ILs.

Sample	Total (wt% AB)	H_2 (wt% AB/ e.q. H_2)	Borazine/ B_2H_6/ NH_3 (wt% AB)	Missing mass (wt% AB)
AB	57.9	10.2/1.58	17.5/3.3/2.2	24.7
AB-EmimCl	31.5	14.5/2.22	11.8/0.5/0.5	4.2
AB-BmimCl	33.1	14.0/2.14	13.3/0.5/0.4	4.9
AB-BmmimCl	31.7	15.1/2.31	11.2/0.4/0.6	4.4

Structural properties

The dehydrogenation process of AB-BmimCl has been discussed by Himmelberger, et al.[22] They claimed that polyborazylene (PB; $\{BNH_x\}_n$, $x < 2$) is formed after dehydrogenation of AB-BmimCl and some other AB-ILs. Indeed, our ^{11}B MAS NMR profile of AB-BmimCl after dehydrogenation shows PB (Fig. 6 (a)). The PB spectrum in this study is different from the previous study[36] since our MAS NMR equipment has a lower magnetic field than that in the previous study.

Since AB-EmimCl and AB-BmmimCl have almost the same ^{11}B MAS NMR profile as that of AB-BmimCl after dehydrogenation, the same material, PB, likely forms after their dehydrogenation (Fig. 6 (b, c)). On the other hand, the ^{13}C MAS NMR and ^{1}H solution NMR show interesting results. The AB-IL mixed

solutions exhibit sharp peaks due to their liquid state while the signals of neat ILs and dehydrogenated AB-ILs are broad due to being solids (Fig. 7). ^{13}C signals at 0 to 60 ppm region are corresponding to branches on the imidazolium rings (methyl, ethyl, and butyl groups) and signals at 110 to 150 ppm correspond to the imidazolium ring.[37] All ^{13}C signals of mixed AB-ILs shift to the higher magnetic fields, especially the branches (butyl and methyl group of $R^1 \sim R^3$, 0 to 60 ppm in fig. 1) of imidazolium ring compared to the neat ILs (each of the bottom profiles of AB-ILs in fig. 7). After dehydrogenation, these peaks shift back to lower magnetic field close to their original position (each of the middle profiles of AB-ILs in fig. 7). However, almost all of these peaks are at slightly higher magnetic field (except for R^1 methyl group in AB-BmmimCl) after dehydrogenation. The methyl CH_3 (R^3) attached to the N atom in BmimCl and R^2 in BmmimCl shifted back relatively less than the other peaks after dehydrogenation.

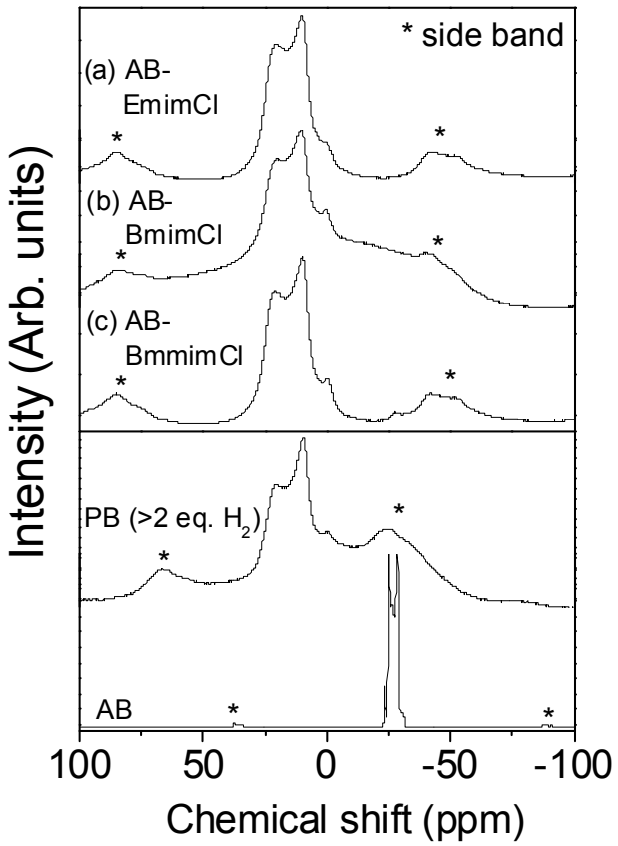

Figure 6. ^{11}B MAS NMR spectra of AB-ILs after dehydrogenation together with AB and PB as references.

The tendencies of shifting higher magnetic field when mixed and shifting back after dehydrogenated also can be seen in ^1H solution NMR in fig. 8. The sharp peaks from 0 to 5 ppm are corresponding to hydrogen atoms of the R^n branches while the peaks from 7 to 10 ppm are corresponding to the hydrogen on the imidazolium ring.[38] AB signals are broadly locates at 0 to 2 ppm (BH_3) and around 4.5 ppm (NH_3).[39] The peaks at Hydrogen atom of R^2 in AB-EmimCl and AB-BmimCl shifts ~1 ppm higher magnetic field than the original position when mixed with AB. After the dehydrogenation, methyl, ethyl, and butyl group signals in ^1H NMR profiles of AB-ILs shift back to close position to neat IL position, except CH_3 groups of R^1 and R^2 in BmmiCl. After dehydrogenation, the exceptions, CH_3 groups of R^1 and R^2, shift slightly higher magnetic field than as mixed. These NMR profiles indicate that the AB and ILs did not react with each other during dehydrogenation, but the structures of ILs after mixing and following dehydrogenation are slightly different from the neat ILs. These profiles also show that the electron densities of the ILs are affected by AB and PB. Cl^- anion interacts strongly with the ILs R^2 = H or CH_3. Upon mixing with AB, this Cl^--R^2 interaction appear to be disrupted based on the NMR data, allowing the stronger hydrogen-bonding AB that can interact both with the R^2 group and the side chains on the imidazolium ring. Following dehydrogenation, AB is removed from this coordinating position as it converts to oligomeric and polymeric PB, resulting in a solid solution of PB and ILs.

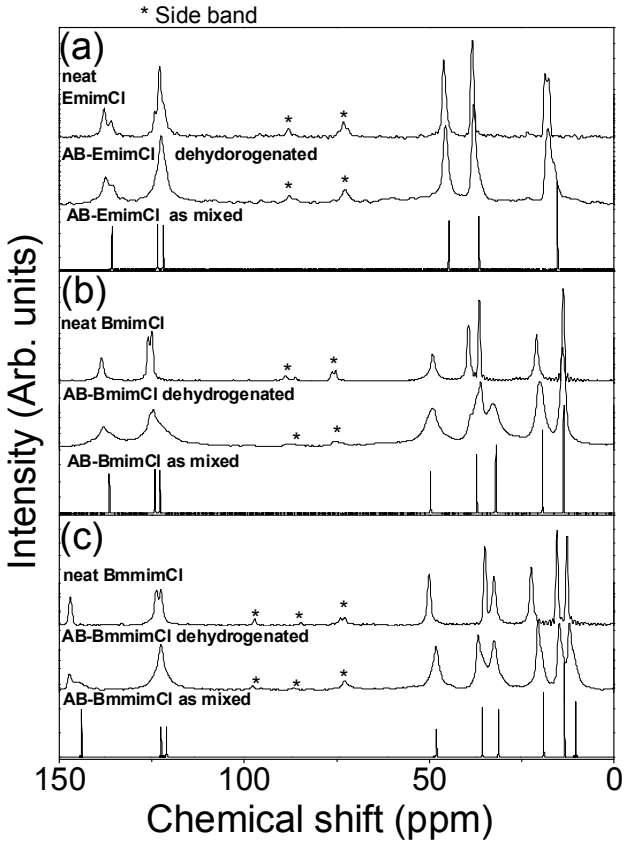

Figure 7. ^{13}C MAS NMR profiles of neat ILs and AB-ILs before and after dehydrogenation.

The geometry of this solid solution is likely to be a layered structure of IL and PB with pi-interactions. This allows the Cl-anion to attain its original interaction with the R^2 group, thus reforming the original IL, but with the weak pi-interactions with the resulting PB that retains slightly altered electronic environments around the imidazolium cations. Further experimental and theoretical approaches are necessary to determine the intermediate and resulting structures accurately.

Conclusions

The basic properties of AB-IL mixtures have been studied,

including dehydrogenation and their resulting structural properties. The resulting properties of the AB-IL eutectics and stability towards dehydrogenation in these liquids lend ILs to be significantly promising in the area of hydrogen storage fuels except solidification after dehydrogenation. The mixtures desorbed small amount of hydrogen with no or quite small amount of impurities. Water content significantly affects the initial stability, and loss of AB fuel occurs due to reaction with the water. AB-ILs dehydrogenate with a peak at ~110 °C and complete desorption of >2 eq. H_2 below 130 °C. Impurity emissions were greatly suppressed by using the IL as the solvent, particularly in the limited release of ammonia. ^{11}B MAS NMR showed that PB forms following dehydrogenation of AB-ILs, and ^{1}H solution and ^{13}C MAS NMR spectra indicate that no reaction occurs between IL and AB, but the IL structures are slightly changed due to the different interactions with AB and PB. The final PB-IL mixture appears to be a solid solution, though more detailed structural studies are required, which would aid in the development of ILs that can maintain a liquid nature post-dehydrogenation, resulting in a liquid fuel before and after use and readily engineered for transportation applications.

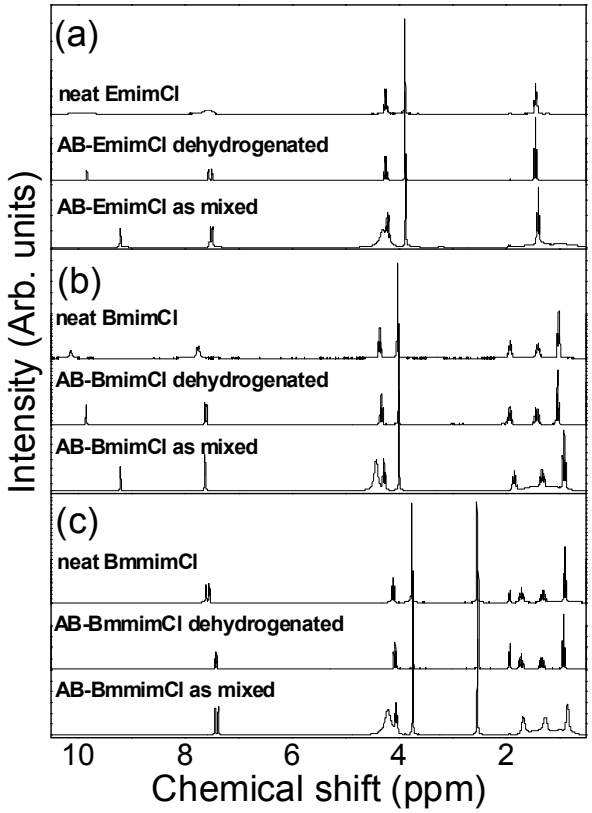

Figure 8. ^{1}H solution NMR profiles of neat ILs and AB-ILs before and after dehydrogenation.

Acknowledgement

This work was supported by the DOE office of EERE (Energy Efficiency and Renewable Energy) under contract numbers NA25396 and DE-EE-0005658.

Notes and references

[a] *Materials Physics and Applications division, Los Alamos National Laboratory, MS J514, Los Alamos National Laboratory, Los Alamos, NM 87544, USA. Fax: +1-505-667-9905; Tel: +1-505-500-2463; E-mail: bldavis@lanl.gov*
[b] *Chemistry Division, Los Alamos National Laboratory, MS J512 Los Alamos National Laboratory, Los Alamos, NM 87545, USA.*
[c] *Department of Mechanical Engineering, Stanford University, 450 Serra Mall, Stanford, California 94305, USA.*

[†] *Faculty of science, University of the Ryukyus, 1 Senbaru, Nishihara, Okinawa 903-0213, Japan. Fax: +81(98)895-8565; Tel: +81(98)895-8535; E-mail: tessui@sci.u-ryukyu.ac.jp*
[‡] *Chemical Sciences and Engineering Division, Argonne National Laboratory, 9700 S. Cass Avenue, Argonne, IL 60439, USA.*
[§] *Department of Physical Sciences, Dixie State University, 225 South 700 East, St. George, UT 84770.*
[‖] *International Research Center for Hydrogen Energy, Kyushu University, 744 Motooka, Nishi-ku, Fukuoka 819-0935 Japan.*
[¶] *State Key Laboratory of Heavy Oil Processing, China University of Petroleum, Beijing 102249, China.*

1 L. Schlapbach, A. Züttel, *Nature*, 2001, **414**, 353.
2. K. Hirose, *Faraday Discuss.*, 2011, **151**, 11.
3. The Department of Energy Hydrogen and Fuel Cells Program Plan, http://www.hydrogen.energy.gov/pdfs/program_plan2011.pdf.
4. D. Anton, T.A. Semelsberger, D. Siegel, and K. Brooks, B. Hardy, 2013 DOE webinar "Hydrogen Storage Materials Requirements", https://www1.eere.energy.gov/hydrogenandfuelcells/webinar_archives_2013.html#date062513.
5. Y.S. Chua, P. Chen, G. Wu, and Z. Xiong, *Chem. Commun.*, 2011, **47**, 5116.
6. F. Baitalow, J. Baumann, G. Wolf, K. Jaenicke-Rößler, and G. Leitner, *Thermochim. Acta*, 2002, **391**, 159.
7. F. Cheng, H. Ma, Y. Li, and J. Chen, *Inorg. Chem.*, 2007, **46**, 788.
8. N. Blaquiere, S. Diallo-Garcia, S.I. Gorelsky, D.A. Black, and K. Fagnou, *J. Am. Chem. Soc.*, 2008, **130**, 14034.
9. B.L. Conley and T.J. Wiliams, *Chem. Commun.*, 2010, **46**, 4815.
10. F.H. Stephens, R.T. Baker, M.H. Matus, D.J. Grant, and D.A. Dixon, *Angew. Chem. Int. Ed.*, 2007, **46**, 746.
11. X.D. Kang, L.P.Ma, Z.Z. Fang, L.L. Gao, J.H. Luo, S.C. Wang, and P. Wang, *Phys. Chem. Chem. Phys.*, 2009, **11**, 2507.
12. Y. Zhang, K. Shimoda, T. Ichikawa, and Y. Kojima, *J. Phys. Chem. C*, 2010, **114**, 14662.
13. M.C. Denney, V. Pons, T.J. Hebden, D.M. Heinekey, and K.I. Goldberg, *J. Am. Chem. Soc.*, 2006, **128**, 12048.
14. D.W. Himmelberger, C.W. Yoon, M.E. Bluhm, P.J. Carroll, L.G.Sneddon, *J. Am. Chem. Soc.*, 2009, **131**, 14101.
15. S. Sepehri, A. Feaver, W.J. Shaw, C.J. Howard, Q.F. Zhang, T. Autrey, G.Z. Cao, *J. Phys. Chem. B*, 2007, **111**, 14285.
16. Z.G. Li, G.S. Zhu, G.Q. Zhu, G.Q. Lu, S.L. Qiu, and X.D. Yao, *J. Am. Chem. Soc.*, 2010, **132**, 1490.
17. R.Q. Zhong, R.Q. Zou, T. Nakagawa, M.T. Janicke, T.A. Semelsberger, A.K. Burrell, R.E. Del Sesto, *Inorg. Chem.*, 2012, **51**, 2278-2730.
18. H.V.K. Diyabalanage, R.P. Shrestha, T.A. Semelsberger, B.L. Scott, M.E. Bowden, B.L. Davis, and A.K. Burrell, *Angew. Chem. Int. Ed.*, 2007, **46**, 8995.
19. Z. Xiong, C.K. Yong, G. Wu, P. Chen, W. Shaw, A. Karkamkar, T. Autrey, M.O. Jones, S.R. Jhonson, P.P. Edwards, and W.I.F. David, *Nat. Mater.* 2008, **7**, 138.
20 D.Y. Kim, H.M. Lee, J.C. Seo, S.K. Shin, and K.S. Kim, *Phys. Chem. Chem. Phys.*, 2010, **12**, 5446.
21. H.V.K. Diyabalanage, T. Nakagawa, R.P. Shrestha, T.A. Semelsberger, B.L. Davis, B.L. Scott, A.K. Burrell, W.I.F. David, K.R. Ryan, M.O. Jones, and P.P. Edwards, *J. Am. Chem. Soc*. 2010, **132**, 11836.
22. D.W. Himmelberger, L.R. Alden, M.E. Bluhm, and L.G. Sneddon, *Inorg. Chem.*, 2009, **48**, 9883-9889.
23. W.R.H. Wright, E.R. Berkeley, L.R. Alden, R.T. Baker, and L.G. Sneddon, *Chem. Commun.*, 2011, **47**, 3177.

24. S. Basu, Y. Zheng, and J.P. Gore, *J. Power Sources*, 2011, **196**, 734-740.
25. J.G. Huddleston, A.E. Visser, W.M. Reichert, H.D. Willauer, G.A. Broker, and R.D. Rogers, *Green Chem.*, 2001, **3**, 156-164
26. A.A. Fannin, D.A. Floreani, L.A. King, J.S. Landers, B.J. Piersma, D.J. Stech, R.L. Vaughn, J.S. Wilkes, and J.L. Williams, *J. Phys. Chem. B*, 1984, **88**, 2614-2621
27. D.M. Fox, W.H. Awad, J.W. Gilman, P.H. Maupin, H.C. De Long, and P.C. Trulove, *Green Chem.*, 2003, **5**, 724-727.
28. A.K. Burrell, R.E. Del Sesto, S.N. Baker, T.M. McCleskey, G.A. Baker, *Green Chem.*, 2007, **9**, 449 - 454.
29. T.A. Semelsberger, 2012 Annual Merit Review Proceedings, http://www.hydrogen.energy.gov/pdfs/review12/st007_semelsberger_2012_o.pdf.
30. W.T. Klooster, T.F. Koetzle, P.E.M. Siegbahn, T.B. Richardson, and R.H. Crabtree, *J. Am. Chem. Soc.*, 1999, **121**, 6337-6343.
31. A.A. Fannin, D.A. Floreani, L.A. King, J.S. Landers, B.J. Piersma, D.J. Stech, R.L. Vaughn, J.S. Wilkes, and J.L. Wiliams, *J. Phys. Chem. B,* 1984, **88**, 2614-2621.
32. J.G.Huddleston, A.E. Visser, W.M. Reichert, H.D. Willauer, G.A. Broker, and R.D. Rogers, *Green Chem.*, 2001, **3**, 156-164.
33. P.A. Hunt and I.R. Gould, *J. Phys. Chem. A*, 2006, **110**, 2269-2282.
34. Glenn Elert, The physics Hypertextbook-Viscosity, http://physics.info/viscosity/
35. A. Yokozeki, M.B. Shiflett, *Ind. Eng. Chem. Res.*, 2007 **46**, 1605-1610.
36. A.C. Stowe, W.J. Shaw, J.C. Linehan, B. Schmid, and T. Autrey, *Phys. Chem. Chem. Phys.*, 2007, **9**, 1831-1836.
37. V. Farmer and T. Welton, *Green Chem*, 2002, **4**, 97-102.
38. A. Bagno, F. D'Amico, G. Saielli, *ChemPhysChem*, 2007, **8**, 873-881.
39. N. Blaquiere, S. Diallo-Garcia, S.I. Gorelsky, D.A. Black, and K. Fagnou, *J. Am. Chem. Soc.*, 2008, **130**, 14034-14035.

Table of Contents

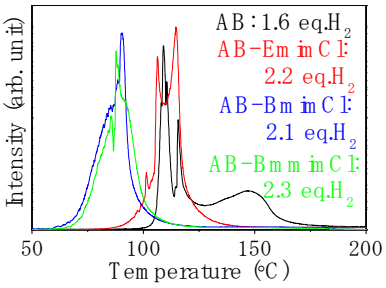

Hydrogen desorption profiles of AB-ILs with H_2 yield.